On the Sensing Mechanism in Carbon Nanotube Chemiresistors

Amin Salehi-Khojin,*,† Fatemeh Khalili-Araghi,‡,§ Marcelo A. Kuroda,⊥ Kevin Y. Lin,† Jean-Pierre Leburton,‡,§,∥ and Richard I. Masel†

†Department of Chemical and Biomolecular Engineering, , ‡Beckman Institute, §Department of Physics, ⊥Department of Computer Science, ∥Department of Electrical and Computer Engineering, and University Of Illinois at Urbana—Champaign, United States

ABSTRACT There has been recent controversy whether the response seen in carbon nanotube (CNT) chemiresistors is associated with a change in the resistance of the individual nanotubes or changes in the resistance of the junctions. In this study, we carry out a network analysis to understand the relative contributions of the nanotubes and the junctions to the change in resistance of the nanotube network. We find that the dominant mode of detection in nanotube networks changes according to the conductance level (defect level) in the nanotubes. In networks with perfect nanotubes, changes in the junctions between adjacent nanotubes and junctions between the contacts and the CNTs can cause a detectable change in the resistance of the nanotube networks, while adsorption on the nanotubes has a smaller effect. In contrast, in networks with highly defective nanotubes, the changes in the resistance of the individual nanotubes cause a detectable change in the overall resistance of a chemiresistor network, while changes in the junctions have smaller effects. The combinational effect is also observed for the case in between. The results show that the sensing mechanism of a nanotube network can change according to the defect levels of the nanotubes, which may explain the apparently contradictory results in the literature.

KEYWORDS: carbon nanotube chemiresistor · carbon nanotube defect · sensing mechanism · electron hopping · network analysis · 1/*f* noise · Poole—Frenkel conduction

Interpenetrating networks of metallic-semiconducting carbon nanotubes (CNTs) have been increasingly used as one of the key electronic materials for new classes of chemiresistors.[1−9] They consist of arrays of nanotubes between two gold contacts and produce a highly sensitive response compared to other solid-state gas chemiresistors. At this point, there is some controversy whether the response arises from the modulation of nanotube themselves, modulation of the junctions between gold and the nanotubes, or modulation of the junctions between two adjacent nanotubes. For example, K. Bradley *et al.*[10] showed that NH_3 mainly interacts with carbon nanotubes themselves. In contrast, N. Peng *et al.*[11] suggested that the modulation of nanotube—metal electrode junctions influence the response to NH_3. In another experiment, Liu *et al.*[12] observed that both nanotube channels and nanotube—gold junctions play a role in the detection process of NH_3.

The objective of our work was to do calculations to see if we can understand why different sets of careful experiments give different results. In particular we were interested in determining whether changes in the properties of the nanotubes could change the dominant sensing mechanism. Recall that Gomez-Navarro *et al.*[13] found that the resistance of a nanotube changes by 3 orders of magnitude as defects form on the nanotube surface. We were interested if such changes were sufficient to switch the dominant mode of sensing.

Our results show that the dominant sensing mechanism is highly dependent on the resistance of the nanotube. In particular, we show that in networks consisting of highly conductive (perfect) nanotubes the chemiresistor response is determined by the junctions between adjacent metal nanotubes and the junctions between the nanotubes and the gold. However, in networks with low conductive (heavily defective) nanotubes, the chemiresistor response is determined by modulations in the resistance of the nanotubes themselves. The combinational effect is also observed for the case in between.

This conclusion arises from a detailed systematic analysis of the network electric transport analysis considering both metallic and semiconducting CNTs and corresponding homogeneous—heterogeneous junctions. We did such an analysis and asked the question, "How do changes in the resistance of the metal nanotubes, the semiconducting nanotubes, and the junctions between them influence the response of a nanotube network?" Our numerical technique is to

*Address correspondence to salehikh@illinois.edu.

Received for review August 11, 2010 and accepted December 15, 2010.

Published online December 27, 2010. 10.1021/nn101995f

vary the resistance of metallic and semiconducting nanotubes and corresponding homogeneous−heterogeneous junctions one at a time within the experimental range and determine the overall change of network conductance. We also considered a similar resistance for junctions between gold electrodes and nanotubes and junctions between two adjacent metallic nanotubes.

In detail, each CNT was modeled as a stick of length L that is randomly positioned on a 2D surface. One end of the tube is positioned randomly on the surface and its other end is determined after picking an arbitrary orientation with a uniform probability distribution between −180 and 180 degrees. Coordinates of the CNT junctions (nodes) are determined, and a connectivity matrix (that identifies pairs of nodes that are connected to each other with a finite resistance) is defined to represent the CNT network. In the produced network, the resistance arises because of two contributions: the resistance of the individual CNT and the resistance of junctions. On the basis of Gomez-Navarro *et al.*'s work[13] we choose three different scenarios in our simulation for CNTs: (i) perfect tube, (ii) slightly defective nanotubes, and (iii) heavily defective nanotubes. The resistance of each tube was calculated using the expression in ref 14 with a prefactor of f ($1 \leq f \leq 1000$)[13] for the defects part as follows:

$$R = f\frac{R_0}{2}\left[1 + \frac{L}{\lambda_{\text{eff}}}\right] \quad (1)$$

in terms of the quantum resistance $R_0 = h/(2e^2)$ (where e is the electron charge and h is Planck's constant) and the effective carrier mean free path λ_{eff}. In the case of metallic CNTs, the effective mean free path used in the computation was on the order of 600 nm after accounting for the contribution of both acoustic and optical phonons.[14] In the case of intrinsic semiconducting nanotubes, their low carrier loading prevents the electrical conduction in the absence of doping, and their effective resistance becomes more than 4 orders of magnitude larger than their metallic counterparts. The junction resistances were assigned to $15.38R_0$ for metal−metal junctions, $33.3R_0$ for semiconducting−semiconducting junctions, and 100 times higher than that of metal−metal for metal−semiconducting junctions.[15] Applying Kirchhoff's laws to the resulting network of resistors, the overall conductance of the network was calculated. The simulations corresponding to a certain network loading were repeated between 300 and 1000 times (depending on the CNT loading), and average values for the conductance of the network over these repetitions are reported.

RESULTS AND DISCUSSION

Figure 1 displays the nanotube networks' conductance obtained from simulation for the nanotube loadings per unit area up to 6 μm^{-2}. This is equivalent to 4 mg/L nanotube in solution, which will be discussed later. We define P as the probability of finding at least one conducting path in the network. The inset of this figure shows the percolation probability of the chemiresistors, P, as a function of the CNT loading. The dependence of network conductivity (σ) on CNT loading obtained from simulation is in accordance with the standard percolation theory described by $\sigma \propto (N - N_c)^{\alpha}$, where N is the volume loading of the nanotube solution, N_c is the critical volume loading of the CNT corresponding to the percolation threshold ($N_c = 1/\pi(4.236/L_{\text{tube}})^2$, and α is a critical fitting exponent. The best fit of $\sigma \propto (N - N_c)^{\alpha}$ to the theoretical curve shown in Figure 1 results in $\alpha = 1.92$, which is close to the theoretical prediction of $\alpha = 1.94$.[16] Here we point out that the simulations performed in this study provide detailed information about nanotube networks, such as distribution of the current among metallic and semiconducting nanotubes, which cannot be accessed from experiment and analytical percolation equations.

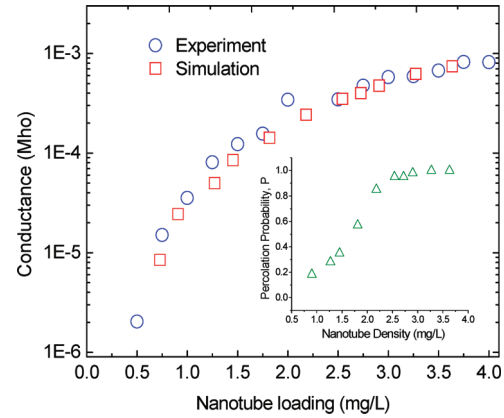

Figure 1. (a) Experimental and simulated conductance vs nanotube loading. The average conductance for the ensemble of networks fits very well to experimental results using a conversion factor of 0.66, the ratio of mass per unit volume of nanotube solution (mg/L) over nanotube loading in unit area (μm^{-2}).

We also did experiments to verify the predictions of the computations. CNT networks shown in Figure 2 were fabricated using liftoff photolithography as described in our previous papers,[17,18] and the conductance shown in Figure 1 was measured. The average conductance measured for the network shows very good agreement with the simulations using a conversion factor of 0.66, the ratio of mass per unit volume of nanotube solution (mg/L) over nanotube loading in unit area (μm^{-2}).

Figure 3 shows the change in overall conductance of a network with equivalent loading of 1 mg/L by separately varying the resistance of the metallic nanotubes, the resistance of the semiconducting nanotubes, the resistance of the junctions between adjacent metal nanotubes, the resistance of junctions between adjacent semiconducting nanotubes, and the resistance of the junctions between adjacent metallic and semiconduct-

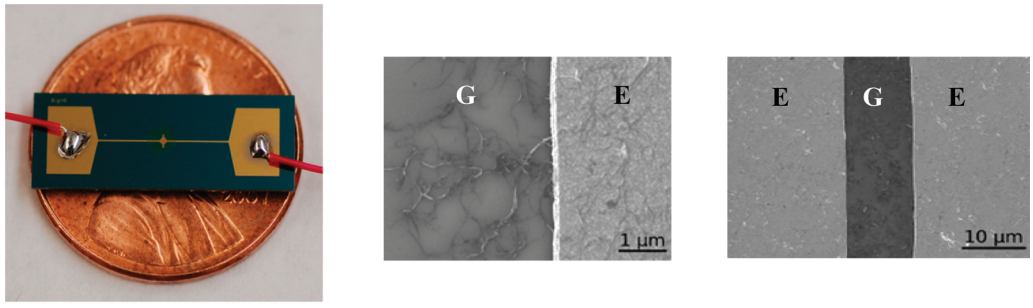

(a)

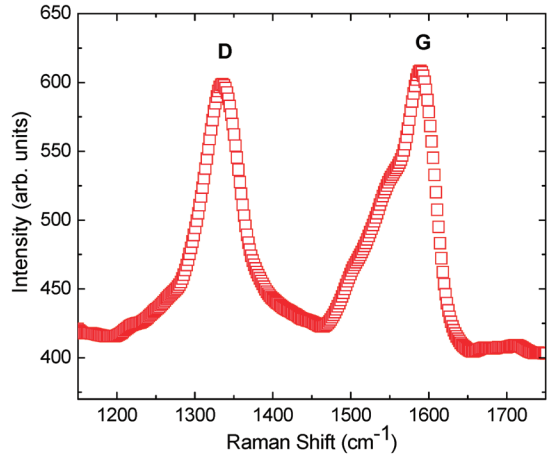

(b)

Figure 2. (a) SEM images of fabricated nanotube chemiresistors. The gap zone and electrodes are labeled G and E in the SEM images, respectively. (b) Display of a typical Raman spectrum of our nanotube chemiresistors (1 mg/L) that include nanotube peaks, which consist of a sp^3-like disorder band (D) around 1340 cm^{-1} and a sp^2-like tangential band (G) around 1590 cm^{-1}. The Raman spectra were obtained using an Ar+ laser operating at 514.5 nm (2.41 eV), a spot size of 50 μm diameter, and 3 mW of power on the sample.

ing nanotubes. We did the analysis for three different conductance levels of nanotubes: (a) perfect nanotubes ($f = 1$ in eq 1), (b) heavily defective nanotubes ($f = 500$), (c) slightly defective nanotubes ($f = 70$). For perfect nanotubes (Figure 3a), we found that if the resistance of the junctions between adjacent metallic nanotubes changes as one might expect if gas adsorbs, there is a large change in the conductance of the network. In contrast variations in the resistance of metallic nanotubes, semiconducting nanotubes, and junctions between two adjacent semiconducting nanotubes and between the adjacent metallic−semiconducting nanotubes have little effect.

By comparison when the nanotubes are highly defective, changes in the resistance of the defective nanotubes have a significant effect on the overall conductance of the network. However, the variations in the resistance of all kinds of junctions have negligible effects. We also see the combinational effects for the case of slightly defective nanotubes, as shown in Figure 3c. These results clearly indicate that different conductance levels of nanotubes yield different sensing mechanisms in a network.

Physically, pristine nanotubes have a very low resistance. In such a case, the resistance of the nanotubes is low compared to the resistance of the junctions between adjacent nanotubes, so large percentage changes in the conductance of the nanotubes (i.e., changes larger than one would expect for gas adsorption) do not produce a significant change in the conduction of the network. The semiconducting nanotubes also have little effect because they have such high resistance that there is little or no current through them. Thus, only changes in the resistance of the junctions, either between adjacent nanotubes or between the nanotubes and the gold, have a significant effect of the resistance on the network.

Defective nanotubes show the opposite effect. Defects can vary the resistivity of the nanotubes by 3 orders of magnitude.[13] In that case the resistance of the nanotubes is large compared to the resistance of the junctions. Hence, the changes in the resistance of the nanotubes have an important effect on the overall conduction of a network.

The analysis above considered only Shottkey−Richardson conduction in the nanotubes (i.e., conduction through the conduction band), but at higher voltages electron transport also occurs *via* Poole−Frenkel conduction if there are defects in the nanotube. If electrons are transported *via* the

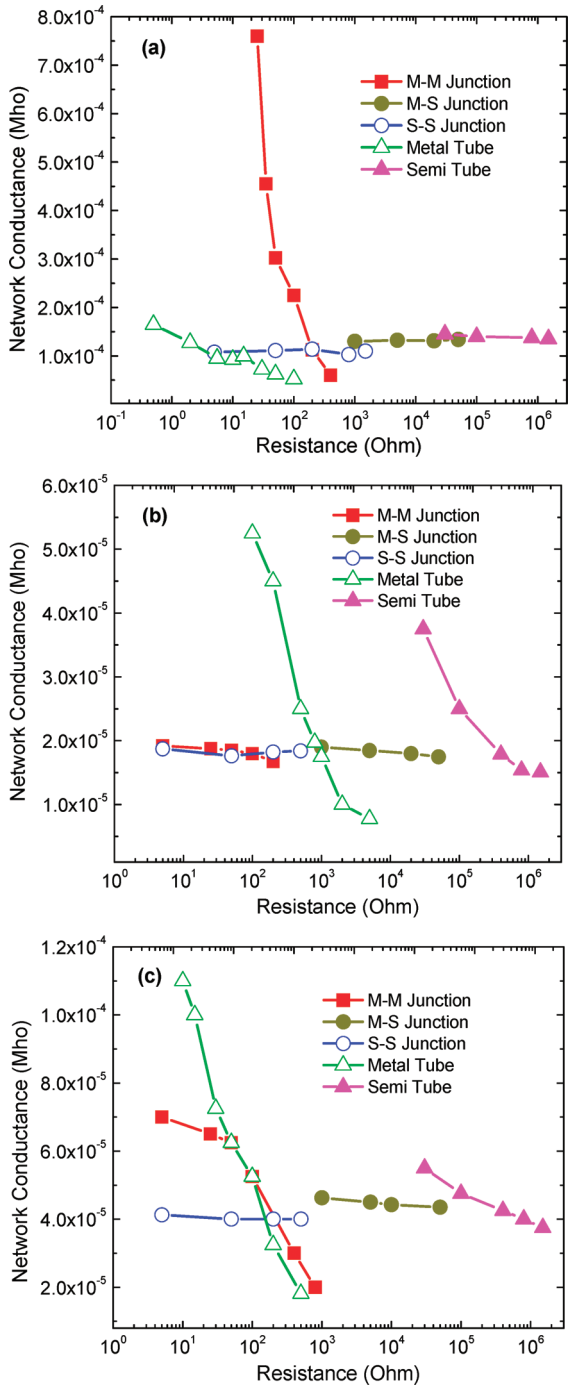

Figure 3. Variation of the nanotube network conductance as a function of the change in the resistance of metallic nanotubes, the change in the resistance of semiconducting nanotubes, and the change in the resistance of junctions between two adjacent nanotubes for the case of (a) perfect nanotube, $f = 1$; (b) highly defective nanotubes, $f = 500$; and (c) slightly defective nanotubes, $f = 70$.

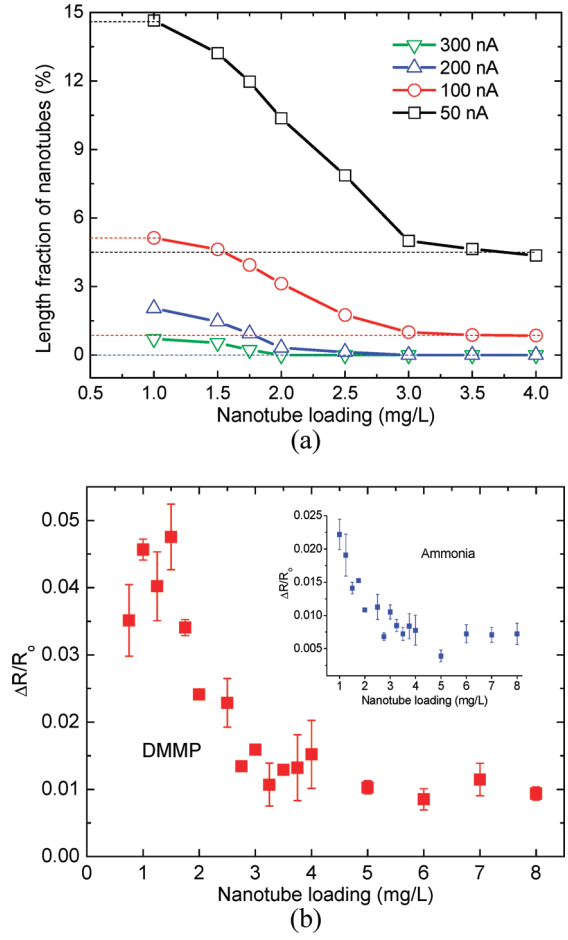

Figure 4. (a) Length fraction of nanotubes that carries specific current vs nanotube loading. 100 nA is the maximum current that the length fraction of all networks is able to carry. Lower currents are not efficient, and higher currents exist only in lower nanotube loadings. (b) Typical normalized response to 10 ppm DMMP gas molecules for nanotube chemiresistors with loadings of 0.75 to 8 mg/L. The inset shows the response to ammonia molecules.

Poole−Frenkel mechanism,[17,19,20] the electron hopping through nanotube defects can inject accumulated charges at the defect sites to the conduction band of the nanotubes, which in turn changes the conductance of the chemiresistor upon gas adsorption. That causes an enhancement in the sensitivity of the nanotubes because the analyte concentration is higher on defects than on pristine regions of the nanotubes. Details of such a mechanism have been explained in ref 17.

To determine the efficient current required for achieving pure electron hopping, we considered the experimental condition where we applied a constant external current and obtained the histogram of currents passing through nanotube segments. Figure 4a shows the histogram results presented in the form of the fraction of nanotubes that carry a specific current at each nanotube loading, while Figure 4b shows the sensitivity of the chemiresistors to adsorption of gas. The details of the experimental section have been explained in refs 17 and 18. In this calculation, we assumed that our network was made of highly defective nanotubes since the Raman spectra shown in Figure 2b show a large density of defects.

It is useful to compare parts a and b of Figure 4. We observe a similar trend for both sensitivity and fraction of nanotubes vs nanotube loading for current equal to

or less than 100 nA. We also observe that there are no nanotube segments at higher loadings that carry currents higher than 100 nA. The results suggest that 100 nA is an upper limit for the minimum current required for an efficient electron-hopping process.

Figure 4 also indicates that the fraction of nanotubes that carry a 100 nA current decreases with the increase in the network loading. This result suggests a similar trend in the electron-hopping distance (or range) vs nanotube loading. If this is the case, thus, one should also expect a similar trend in the charge fluctuation and consequently in the 1/*f* noise level. To check this hypothesis, we measured the 1/*f* noise level of our chemiresistors at three different applied currents for different nanotube loadings. Results are displayed in Figure 5. We attribute the increased 1/*f* noise level at lower nanotube loadings to higher charge fluctuations in these networks due to higher extent of electron-hopping processes. A diminished trend of 1/*f* noise with network loading is also consistent with the reduction in the electron-hopping distance (or range), as shown in Figure 4. The results indicate that the electron-hopping mechanism in Poole−Frenkel conduction well describes the sensitivity and noise level in highly defective nanotube chemiresistors.

To summarize, we performed network simulation to differentiate the sensing mechanism in nanotube chemiresistors. We found that the change in the resistance of nanotubes can modify the dominant detection mechanism in nanotube chemiresistors. Our results showed that networks with highly defective nanotubes

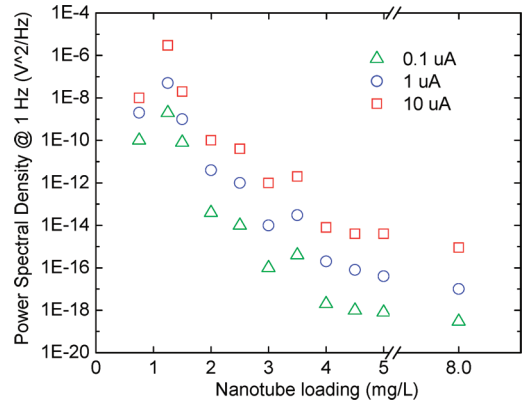

Figure 5. Measured noise density for nanotube chemiresistors with nanotube loadings ranging from 0.75 to 8 mg/L at three applied electric currents. The maximum noise level is at 1 mg/L. The noise level decreases with the network loading and then stays fairly constant. A similar trend was observed in Figure 4a and b.

were influenced only by change in the resistance of the nanotube themselves, while networks with pristine nanotubes were modulated only by modulation of the resistance of junctions. Clearly, in the latter case, among junctions between a gold electrode and nanotubes, and junctions between adjacent metallic nanotubes, the one with lower conductance dominates the overall conductance of nanotube networks. Our results explain how seemingly identical studies done carefully on different nanotubes and with different fabrication techniques can reach different conclusions on the dominant sensing mechanism in nanotube networks, as reported by Bradley *et al.*,[10] Peng *et al.*,[11] and Liu *et al.*[12]

METHODS

Fabrication and Design of the Chemiresistor. Nanotube chemiresistors were fabricated using standard lift-off photolithography. A silicon substrate with a thermal oxide layer (500/0.6 μm Si/SiO_2) was patterned with chrome and gold (17/100 nm Cr/Au) for source and drain electrodes separated by a 6 μm gap. 3-Aminopropyltriethoxysilane (APTES, 1%) (Gelest, Inc.) was utilized as a supportive coating to enhance the interaction between the SWNT film and the silicon substrate.

SWNT Preparation and Deposition on Silicon Substrate. A highly concentrated SWNT suspension (400 mg/L) was made from 10 mg of SWNT powder (Unidym, High Purity HIPCO) and 1% (w/v) sodium dodecyl sulfate (SDS) in water. Multiple sets of 10 min, low-powered ultrasonication (at 40% power and 90% frequency), 1 h stirring, and 3 h centrifugation (at 2800*g* or 4100 rpm) were performed to homogenize and uniformly disperse the suspension. The highly concentrated, homogeneous SWNT suspension was then diluted to a selected concentration (mg/L) in a 25 mL solution before being vacuum filtered with mixed cellulose ester (MCE) membranes (Millipore, 0.22 μm pore size). After the SWNT was successfully deposited onto the membranes, the wet MCE-SWNT membrane was dried for at least 2 h under 381 mmHg gauge pressure before multiple rinsings with approximately 80 mL of purified and deionized water (Millipore, Milli-Q water). Multiple rinsing was intended to completely remove the SDS residue from the MCE-SWNT membrane. Finally, a stamp technique was used to transfer homogeneous, randomly aligned CNT films to the APTES-treated silicon surface.

Acknowledgment. This work was supported by grants from Cbana Laboratories and Dioxide Materials. The authors would like to thank Dr. Behnam for his useful comments on nanotube network design.

REFERENCES AND NOTES

1. Kong, J.; Franklin, N. R.; Zhou, C.; Chapline, M. G.; Peng, S.; Cho, K.; Dai, H. Nanotube Molecular Wires as Chemical Sensors. *Science* **2000**, *287*, 622–625.
2. Lee, C. Y.; Sharma, R.; Radadia, A. D.; Masel, R. I.; Strano, M. S. On-Chip Micro Gas Chromatograph Enabled by a Noncovalently Functionalized Single-Walled Carbon Nanotube Sensor Array13. *Angew. Chem.* **2008**, *120*, 5096–5099.
3. Novak, J. P.; Snow, E. S.; Houser, E. J.; Park, D.; Stepnowski, J. L.; McGill, R. A. Nerve Agent Detection Using Networks of Single-Walled Carbon Nanotubes. *Appl. Phys. Lett.* **2003**, *83*, 4026–4028.
4. Peng, G.; Tisch, U.; Haick, H. Detection of Nonpolar Molecules by Means of Carrier Scattering in Random Networks of Carbon Nanotubes: Toward Diagnosis of Diseases via Breath Samples. *Nano Lett.* **2009**, *9*, 1362–1368.
5. Robinson, J. A.; Snow, E. S.; Badescu, S. C.; Reinecke, T. L.; Perkins, F. K. Role of Defects in Single-Walled Carbon Nanotube Chemical Sensors. *Nano Lett.* **2006**, *6*, 1747–1751.
6. Robinson, J. A.; Snow, E. S.; Perkins, F. K. Improved Chemical Detection Using Single-Walled Carbon

Nanotube Network Capacitors. *Sensors and Actuators, A: Phys.* **2007**, *A135*, 309–314.
7. Snow, E. S.; Perkins, F. K.; Houser, E. J.; Badescu, S. C.; Reinecke, T. L. Chemical Detection with a Single-Walled Carbon Nanotube Capacitor. *Science* **2005**, *307*, 1942–1945.
8. Vichchulada, P.; Zhang, Q.; Lay, M. D. Recent Progress in Chemical Detection with Single-Walled Carbon Nanotube Networks. *Analyst (Cambridge, U. K.)* **2007**, *132*, 719–723.
9. Zribi, A.; Knobloch, A.; Rao, R. CO_2 Detection Using Carbon Nanotube Networks and Micromachined Resonant Transducers. *Appl. Phys. Lett.* **2005**, *86*, 203112/1–203112/3.
10. Bradley, K.; Gabriel, J. C. P.; Star, A.; Gruner, G. Short-Channel Effects in Contact-Passivated Nanotube Chemical Sensors. *Appl. Phys. Lett.* **2003**, *83*, 3821–3823.
11. Peng, N.; Zhang, Q.; Chow, C. L.; Tan, O. K.; Marzari, N. Sensing Mechanisms for Carbon Nanotube Based NH_3 Gas Detection. *Nano Lett.* **2009**, *9*, 1626–1630.
12. Liu, X.; Luo, Z.; Han, S.; Tang, T.; Zhang, D.; Zhou, C. Band Engineering of Carbon Nanotube Field-Fffect Transistors via Selected Area Chemical Gating. *Appl. Phys. Lett.* **2005**, *86*, 1–3.
13. Gomez-Navarro, C.; Pablo, P. J. D.; Gomez-Herrero, J.; Biel, B.; Garcia-Vidal, F. J.; Rubio, A.; Flores, F. Tuning the Conductance of Single-Walled Carbon Nanotubes by Ion Irradiation in the Anderson Localization Regime. *Nat. Mater.* **2005**, *4*, 534–539.
14. Kuroda, M. A.; Leburton, J. P. High-Field Electrothermal Transport in Metallic Carbon Nanotubes. *Phys. Rev. B* **2009**, *80*, 165417.
15. Fuhrer, M. S.; Nygard, J.; Shih, L.; Forero, M.; Yoon, Y.-G.; Mazzoni, M. S.; Choi, H. J.; Ihm, J.; Louie, S. G.; Zettl, A.; *et al.* Crossed Nanotube Junctions. *Science* **2000**, *288*, 494–497.
16. Stauffer, G. *Introduction to Percolation Theory*; Taylor & Francis: London, 1985.
17. Salehi-Khojin, A.; Field, C. R.; Yeom, J.; Shannon, M. A.; Masel, R. I. Sensitivity of Nanotube Chemical Sensors at the Onset of Poole-Frenkel Conduction. *Appl. Phys. Lett.* **2010**, *96*, 163110–163113.
18. Salehi-Khojin, A.; Lin, K. Y.; Field, C. R.; Masel, R. I. Nonthermal Current Stimulated Desorption of Gases from Carbon Nanotubes. *Science* **2010**, *329*, 1327–1330.
19. Jombert, A. S.; Coleman, K. S.; Wood, D.; Petty, M. C.; Zeze, D. A. Poole-Frenkel Conduction in Single Wall Carbon Nanotube Composite Films Built Up by Electrostatic Layer-by-Layer Deposition. *J. Appl. Phys.* **2008**, *104*, 094503/1–094503/7.
20. Suehiro, J.; Imakiire, H.; Hidaka, S.-i.; Ding, W.; Zhou, G.; Imasaka, K.; Hara, M. Schottky-Type Response of Carbon Nanotube NO_2 Gas Sensor Fabricated onto Aluminum Electrodes by Dielectrophoresis. *Sens. Actuators, B* **2006**, *B114*, 943–949.